Journal of Electrical Engineering, Vol. 75, No. 3, 2024, pp. 181-191

sciendo

PAPERS

# Artificial neural network-based method for overhead lines magnetic flux density estimation

**Ajdin Alihodžić, Adnan Mujezinović, Emir Turajlić**

This paper presents an artificial neural network (ANN) based method for overhead lines magnetic flux density estimation. The considered method enables magnetic flux density estimation for arbitrary configurations and load conditions for single-circuit, multi-circuit, and also overhead lines that share a common corridor. The presented method is based on the ANN model that has been developed using the training dataset that is produced by a specifically designed algorithm. This paper aims to demonstrate a systematic and comprehensive ANN-based method for simple and effective overhead lines magnetic flux density estimation. The presented method is extensively validated by utilizing experimental field measurements as well as the most commonly used calculation method (Biot - Savart law based method). In order to facilitate extensive validation of the considered method, numerous magnetic flux density measurements are conducted in the vicinity of different overhead line configurations. The validation results demonstrate that the used method provides satisfactory results. Thus, it could be reliably used for new overhead lines' design optimization, as well as for legally prescribed magnetic flux density level evaluation for existing overhead lines.

Keywords: artificial neural network, field measurements, magnetic flux density, overhead lines, validation

## 1 Introduction

Due to the popularization of artificial intelligence, as well as the advantages of its use, new methods based on the use of artificial intelligence techniques are developed in various areas of human activity [1, 2]. The electric power systems (EPS) are no exception, and numerous artificial intelligence-based methods proved themselves as potentially most effective solutions for different challenges in power systems control, protection, planning, operation and forecasting [3, 4].

The magnetic field plays an essential role in various applications in industry, science, medicine and everyday life. Therefore, various methods are being developed for determining the value and distribution of the magnetic field in space, from analytical and numerical calculation methods to field measurements or device prototype measurements [5-9]. In recent years, the possibility of applying artificial intelligence in electromagnetism has been intensively considered in order to facilitate these processes. Furthermore, the field of electromagnetism is precisely described by Maxwell's equations, and it is an excellent application for testing new artificial intelligence-based methods [10].

During the last decades, there has been an increase in the interest of the public as well as the professional community in the effects of low-frequency magnetic fields on living beings [11-13]. Among all factors that drive the research of new methods, the regulation that in many countries prescribes the necessity of determining the distribution of magnetic fields near power facilities stands out [14-19].

When it comes to the regulation regarding exposure limitations, this topic is a differently treated in various countries. The usual differentiation of exposure limitations is to public exposure and occupational exposure. Some international organizations such as International Commission on Non-Ionizing Radiation Protection (ICNIRP), Institute of Electrical and Electronics Engineers (IEEE), European Parliament and European Council also issued documents regarding this topic. The guidelines issued by ICNIRP in 2010, for limiting exposure to time-varying electric and magnetic fields (1 Hz to 100 kHz) defines that the reference values, unperturbed root mean square (RMS), for general public exposure to magnetic field of frequency 50 Hz are 200 μT, and for the occupational exposure 1000 μT [15]. The IEEE standard C95.1-2019, defines that for the 50 Hz magnetic fields reference values, RMS quantities, are 904 μT in the case of the persons in the unrestricted environments, and 2710 μT for the case of persons in the restricted environment. These values refer to the exposure of the head and torso. For the exposure of the limbs, reference exposure values are significantly higher [19]. Directive of the European Council on the limitation of the exposure of the general public to electromagnetic

University of Sarajevo, Faculty of Electrical Engineering, Sarajevo, Bosnia and Herzegovina
ajdin.alihodzic@etf.unsa.ba, adnan.mujezinovic@etf.unsa.ba, eturajlic@etf.unsa.ba

https://doi.org/10.2478/jee-2024-0022, Print (till 2015) ISSN 1335-3632, On-line ISSN 1339-309X

fields from the 1999 defines the limit value 100 μT for exposure to 50 Hz magnetic field [14]. On the other hand, European Parliament passed a directive regarding exposure to of the workers to the risks arising from physical agents. This directive defines the limit values as 1000 μT in the case of low action level, and 6000 μT for the case of high action level exposure of workers [17].

Some countries are incorporated into their legislation the limit values recommended by some of the above-mentioned organizations, whilst others have defined on their own different limit values. Furthermore, in some countries the reference values are defined in the form of recommendations of the governmental organizations or voluntarily agreed by the electricity utilities [18, 20]. In the author's country, Bosnia and Herzegovina, there is no legislation regarding the exposure levels to the electric and magnetic fields.

Determination of the magnetic flux density distribution near overhead lines is usually performed by measurements or calculations applying the Biot-Savart (BS) law-based method or numerical methods for solving Maxwell's equations [21-25]. Recently, ANNs [26-28] and genetic algorithm [29] have been applied for the overhead lines' electric and magnetic field determination. Among the different types of ANNs used for this purpose, the Multi-Layer Perceptron (MLP) type ANN stood out as the most effective and most commonly used [30-32].

This paper considers a method that utilizes ANN for magnetic flux density estimation in the vicinity of overhead lines. The considered method enables magnetic flux density estimation for arbitrary configurations of single-circuit, multi-circuit, and overhead lines that share a common corridor, without restrictions regarding their load condition and voltage level. The ANN model training is performed based on the dataset generated by utilizing an algorithm developed especially for that purpose. Validation of the ANN-based method is carried out based on the extensive field measurements results in the vicinity of single-circuit, multi-circuit, and overhead lines that share a common corridor. Method performance quantification is performed based on a huge amount of data obtained by experimental magnetic flux density field measurements

The rest of the paper is organized as follows. The ANN-based method for magnetic flux density estimation is discussed in Section 2. Extensive validation of the ANN-based method based on different overhead line configurations is provided in Section 3. Discussion is presented in Section 4. Section 5 concludes the paper.

## 2 Artificial neural network-based method

The ANN-based method for magnetic flux density estimation in the proximity of overhead lines is considered in this paper. This method aims to provide accurate magnetic flux density estimates for both single-circuit and multi-circuit overhead lines, irrespective of the total number of three-phase circuits. A constant number of parameters is needed to adequately describe each three-phase overhead line circuit for magnetic flux density determination purposes. That makes the application of ANNs for multi-circuit overhead lines quite challenging. The considered method provides the response to these challenges and enables simple and efficient magnetic flux density estimation for single-circuit and multi-circuit overhead lines, as well as overhead lines that share common corridors. A significant feature of this method is that only one ANN model is used, i.e. model developed for single-circuit overhead lines, and it does not use a separate ANN model for multi-circuit overhead lines. The input features are carefully selected to enable efficient ANN model training. The ANN model is developed for single-circuit overhead line configurations, but the method presented in this paper allows it to be applied for the estimation of magnetic flux density for the arbitrary configurations of single-circuit, multi-circuit, and overhead lines that share common corridors.

The architecture of the ANN model used for magnetic flux density estimation for arbitrary configurations of single-circuit overhead lines consists of an input layer with 6 inputs, 4 hidden layers with 20 neurons each, and an output layer with 4 outputs. The tan-sigmoid activation function is used for hidden layer neurons [31]. To facilitate effective training of the ANN model, particular attention is placed on selecting the appropriate input features and preparation of an adequate training dataset.

The ANN input parameters represent the spatial coordinates of the three-phase circuit phase conductors $(x_i, y_i)$ $i = 1,2,3$ of overhead line in a 2D coordinate system. It is important to emphasize that the coordinate system, associated with ANN, is defined so that the central phase conductor is located on its ordinate, i.e. $x_1 = 0$, so this data is not used as an ANN input parameter. Therefore, the horizontal distances of the remaining two-phase conductors from the coordinate system ordinate, $x_2$ and $x_3$, and the heights of all phase conductors $y_1, y_2, y_3$ are ANN input parameters. The sixth input parameter represents the horizontal distance of the observation point $x$ from the coordinate system ordinate. All observation points are located at a height of $y = 1$ m above the ground surface, so this information

is not presented to the ANN either. The considered height of the observation points is selected according to the IEC 62110:2009 [33], and IEEE Std 644-2019 [34]. However, the ANN model can also be trained to produce outputs associated with the other heights of observation points. The output parameters of the ANN model are the real and imaginary parts of the magnetic flux density $x$ and $y$ (spatial) vector components at the observation point.

Data collection and preparation is an important step in the development of an ANN model. Considering the need for a dataset consisting of a large number of different configurations of overhead lines, the authors of this paper developed and presented in [28] an algorithm for generating configurations of overhead lines. Based on the algorithm [28], for the purposes of training the ANN model used in this paper, 200,000 different configurations of three-phase single-circuit overhead lines were generated. The configurations are generated in a way to represent the real configurations of overhead lines as authentically as possible. A detailed explanation of the algorithm for overhead line configurations generation can be found in [28]. The scaled conjugate gradient algorithm is utilized for the ANN model training [35].

In order to complete the dataset for ANN training, it is necessary to specify target values for each sample in the training dataset. Target values were obtained by calculating the real and imaginary parts of the magnetic flux density vector spatial components for each generated configuration [31]. The calculations were made using the BS law-based method [36], for observation points 1 m apart, in the range from –100 m to +100 m in relation to the coordinate system ordinate. The observation points are located at a height of 1 m. All calculations were made assuming a constant reference value of the phase current $I_R = 100$ A [28].

## 2.1 Estimation for single-circuit overhead lines

Having developed the ANN model, magnetic flux density estimation for single-circuit overhead lines is a relatively simple procedure, graphically illustrated in Fig. 1. The input parameters to the ANN model are the geometric coordinates of phase conductors and the horizontal distances of the observation points from the coordinate system ordinate. ANN model provides the real and imaginary parts of the magnetic flux density vector spatial components at its output. The ANN model is developed under the assumptions of the reference phase current. Thus, the ANN model outputs need to be appropriately scaled to produce the magnetic flux density estimates associated with the actual overhead line load. Once, the magnetic flux density vector spatial components, corresponding to the actual overhead line load, are known resultant magnetic flux density value can be determined. A detailed explanation, together with governing equations for adjustment of magnetic flux density vector spatial components to actual overhead line load, and resultant value calculation can be found in Section 2.2.

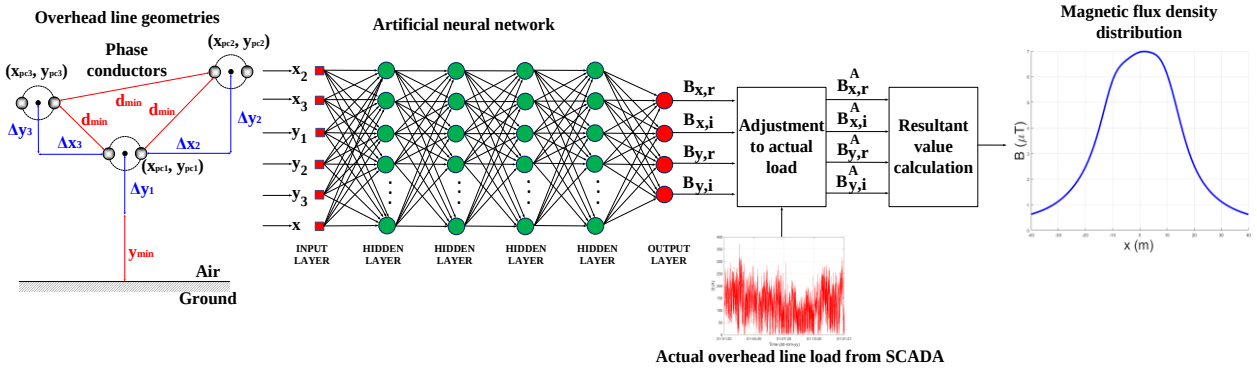


**Fig. 1.** Estimation procedure for single-circuit overhead lines

## 2.2 Estimation for multi-circuit overhead lines

The application of the considered method for magnetic flux density estimation, in the vicinity of multi-circuit and overhead lines that share a common corridor, is based on the use of the ANN model that has been developed for the single-circuit overhead lines. In the case of multi-circuit overhead lines, all individual three-phase circuits need to be identified first. In the next step, for each identified three-phase circuit, the real and imaginary values of the magnetic flux density spatial components are estimated independently based on the single-circuit ANN model.

Multi-circuit overhead lines are often designed in such a manner that it has multiple geometrically identical or symmetrical three-phase circuits. If some of the overhead lines within the same corridor or some of

the multi-circuit overhead line three-phase circuits are geometrically identical or symmetrical to each other, the efficiency of the magnetic flux density determination can be further improved by exploiting the afore-mentioned properties. In such cases, using the ANN model to estimate the magnetic flux density for only one of those, identical or symmetrical, three-phase circuits is sufficient. The magnetic flux density distribution corresponding to identical or symmetrical three-phase circuits can be obtained by some post-processing steps. These steps are based on simple mathematical operations, that are applied to the results obtained for the first three-phase circuit. If geometrically identical circles are considered, it is enough to translate the results along the abscissa. If, on the other hand, three-phase circuits that are symmetrical around the overhead line axis are considered, it is necessary to rotate all the results obtained by the ANN of this coordinate system ordinate and to change the sign of the real and imaginary parts of the magnetic flux density vector $y$ spatial component [31]. When all individual three-phase circuits are geometrically different, the magnetic flux density is estimated individually for each of them.

### *2.2.1 Coordinate system transformations*

As mentioned earlier, in the ANN training dataset, the coordinate system is defined so that the central phase conductor is located on its ordinate in all cases. When considering several overhead lines sharing the common corridor, and/or multi-circuit overhead lines, it is not possible to define a coordinate system so that the central phase line of each individual three-phase circuit is located on the coordinate system ordinate. Therefore, in order to overcome this limitation and determine accurate results regardless of the number and configuration of individual three-phase circuits, it is necessary to define unique (global) coordinate system and coordinate systems for individual three-phase circuits (local). The position of the ordinate of the global coordinate system can be arbitrarily chosen anywhere on the considered lateral profile. On the other hand, the abscissa of the global coordinate system is always defined to coincide with the ground-air boundary.

The local coordinate system for each of the considered three-phase circuits is defined so its ordinate coincides with the central phase conductor of that three-phase circuit. In relation to the global coordinate system, all considered local coordinate systems are shifted only along the abscissa. Therefore, after estimation of the real and imaginary parts of magnetic flux density spatial components for individual three-phase circuits, it is necessary to translate them along the abscissa. For the local coordinate systems placed right, with regard to the global coordinate systems ordinate, the ANN outputs should be translated to the left. Analogously for those placed on the left side, the ANN outputs should be translated to the right. The shifting distance is equal to the distance between the local and global system ordinates [28].

The single-circuit overhead line represents the special case where the centers of the global and local coordinate systems coincide, that is, its local coordinate system is actually also the global coordinate system.

### *2.2.2 Adjustment to actual overhead line load*

Observing the ANN input parameters, it can be noted that the phase current is not one of the parameters presented to the ANN during the training and estimation procedures. The property of linear depen-dence of the overhead lines' magnetic flux density spatial components on the value of the phase current [28, 37] was used. In that way, the magnetic flux density values that correspond to actual overhead lines' loads are obtained. Therefore, the real and imaginary values of the magnetic flux density vector spatial components at an arbitrary observation point with coordinates $(x, y)$ can be determined by applying the following equations:

$$B_{x,r}^{A,n}(x,y) = B_{x,r}^{n}(x,y) \cdot \frac{I_A^n}{I_R} \tag{1}$$

$$B_{x,i}^{A,n}(x,y) = B_{x,i}^{n}(x,y) \cdot \frac{I_A^n}{I_R} \tag{2}$$

$$B_{y,r}^{A,n}(x,y) = B_{y,r}^{n}(x,y) \cdot \frac{I_A^n}{I_R} \tag{3}$$

$$B_{y,i}^{A,n}(x,y) = B_{y,i}^{n}(x,y) \cdot \frac{I_A^n}{I_R} \tag{4}$$

where $(x, y)$ represents coordinates of the considered point in the global coordinate system, $B_{x,r}^{A,n}(x,y)$, $B_{x,i}^{A,n}(x,y)$, $B_{y,r}^{A,n}(x,y)$, $B_{y,i}^{A,n}(x,y)$ are actual magnetic flux density spatial components real and imaginary parts generated by $n$-th circuit, $B_{x,r}^{n}(x,y)$, $B_{x,i}^{n}(x,y)$, $B_{y,r}^{n}(x,y)$, $B_{y,i}^{n}(x,y)$ are magnetic flux density spatial components real and imaginary parts associated with $n$-th circuit for reference current, $I_A^n$ denotes $n$-th circuit actual current and $I_R$ is the reference current.

### *2.2.3 Results integration and resultant magnetic flux density calculation*

After determining the real and imaginary parts of the magnetic flux density vector spatial components, corresponding to the actual load of all individual three-phase circuits, it is necessary to integrate the results associated with each three-phase circuit. Determination

of the magnetic flux density vector spatial components' resultant values, summing up the contributions of all individual three-phase circuits are performed by the following equations:

$$\underline{B}_x^R(x,y) = \sum_{n=1}^{N} B_{x,r}^{A,n}(x,y) + j \cdot \sum_{n=1}^{N} B_{x,i}^{A,n}(x,y) \quad (5)$$

$$\underline{B}_y^R(x,y) = \sum_{n=1}^{N} B_{y,r}^{A,n}(x,y) + j \cdot \sum_{n=1}^{N} B_{y,i}^{A,n}(x,y) \quad (6)$$

where $\underline{B}_x^R(x,y)$ and $\underline{B}_y^R(x,y)$ are resultant values of magnetic flux density spatial components in observation point with coordinates $(x,y)$ that include the contributions of all three-phase circuits. $N$ denotes the total number of considered individual three-phase circuits.

The estimated magnetic flux density value in the observation point with coordinates $(x,y)$ is defined as:

$$\hat{B}(x,y) = \sqrt{|\underline{B}_x^R(x,y)|^2 + |\underline{B}_y^R(x,y)|^2} \quad (7)$$

where $\hat{B}(x,y)$ is the estimated magnetic flux density resultant value.

## 3 Method validation

Validation of the considered ANN-based method for the overhead lines magnetic flux density estimation was made by comparing the results obtained from its application with the field measurements results, and BS law-based method calculation results. The comparison was made by applying the considered ANN-based method, as well as the calculation method, for each overhead line for which measurements were made. Experimental magnetic flux density field measurements are performed in a way that provisions of relevant standards are satisfied [33, 34, 38]. The magnetic flux density measurements are performed over the lateral profiles under overhead lines. The considered lateral profiles are positioned near the centre of the span between two adjacent overhead line towers. These positions of the lateral profiles are selected since the highest magnetic flux density values are expected to be measured there. The measurements are performed at the points of the lateral profiles that are 1 m mutually apart, and at the height of 1 m above the ground surface. The measurements are performed utilizing the NARDA ELT 400 Exposure Level Tester with the three-axis isotropic standard-compliant 100 cm² probe for the RMS and peak value detection. The used instrument enables magnetic flux density measurements in the frequency range from 1 Hz to 400 kHz with a resolution of 1 nT. The magnetic flux density RMS value displayed by the instruments is calculated taking into account the RMS values of all three measurement axes [39]. Since the reference values are defined as the RMS magnetic flux density values, all presented magnetic flux density results are RMS values. Simultaneously to magnetic flux density measurements, conductors' height measurements are performed, and phase current fluctuations are recorded on the SCADA system. The measurements of conductors' height are performed with the cable height meter Suparule model 600.

### 3.1 Single-circuit overhead line

The first considered case represents a 400 kV single-circuit overhead line that connects substation (SS) Sarajevo 10 with SS Sarajevo 20. The considered overhead line was made with a horizontal arrangement of phase conductors. The earth's surface on which the measurements were made can be considered approximately flat. The considered overhead line configuration, at the location of magnetic flux density measurements, is shown in Fig. 2.

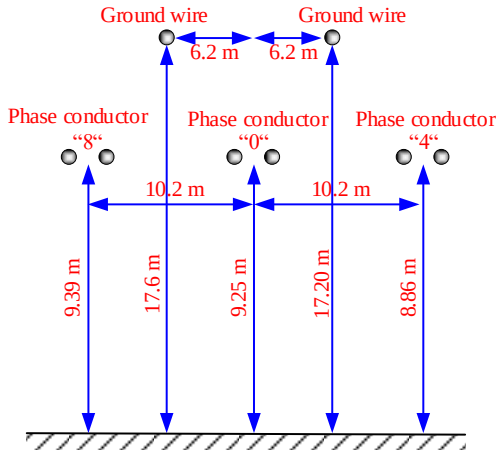


**Fig. 2.** Configuration of 400 kV overhead line SS Sarajevo 10 - SS Sarajevo 20

The magnetic flux density distributions are obtained over the lateral profile from –40 m to + 40 m, in reference to the overhead line axis. Overhead line phase current fluctuations during the measurements are shown in Fig. 3. Phase current used as the input parameter for magnetic flux density determination utilizing the ANN-based method, and BS law-based method is $I_{RMS}$=109.58 A.

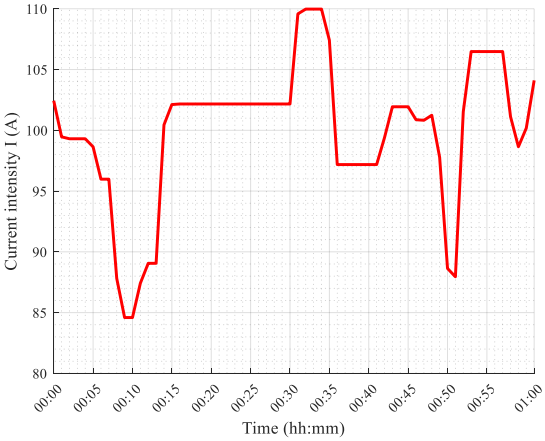


**Fig. 3.** Considered single-circuit overhead line phase current during the measurements

Magnetic flux density results obtained by field measurements, ANN-based method, and BS law-based calculation method under considered overhead line are shown in Fig. 4.

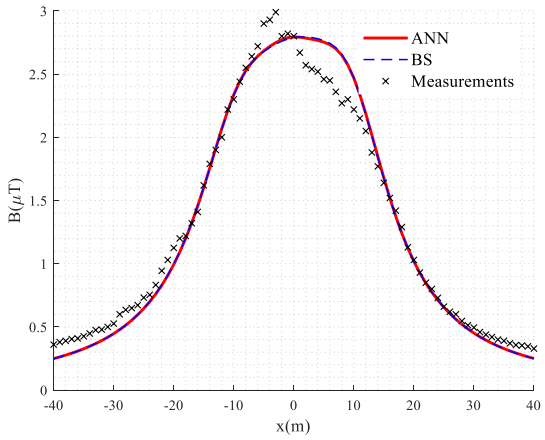


**Fig. 4.** Magnetic flux density distribution for overhead line SS Sarajevo 10 - SS Sarajevo 20

Results given in Fig. 4 demonstrate that in the case under consideration, there is a close agreement between the results obtained by ANN-based method and BS law-based calculations. The level of agreement among these different approaches indicates a degree of reliability and confidence in the considered ANN-based method. Minor deviations are noticeable between the results obtained by these methods and the measured values.

## 3.2 Single-circuit and multi-circuit overhead lines that share common corridor

This section presents the magnetic flux density analysis in the vicinity of a single-circuit 400 kV overhead line that shares a common corridor with a double-circuit 110 kV overhead line. Overhead lines, of 110 kV rated voltage, that connects SS Sarajevo 1 with SS Sarajevo 18, and SS Sarajevo 1 with SS Sarajevo 20, are guided on common towers for a significant part of their corridors, forming a double-circuit overhead line. Furthermore, considered 2×110 kV overhead line is on one part of their corridor parallel with the single-circuit 400 kV overhead line. At the place where the magnetic flux density measurements were made, the distance between the axes of the considered overhead lines is 59 m. The configurations of the considered 400 kV and 2×110 kV overhead lines are shown in Fig. 5.

Since three different three-phase circuits are considered in this case, phase current fluctuations are even more interesting. These fluctuations for overhead lines that share a common corridor are shown in Fig. 6.

Phase current values $I_{RMS}$ = 149.62 A for SS Sarajevo 10 - Sarajevo 20, $I_{RMS}$ = 40.24 A for SS Sarajevo 1 - Sarajevo 18, and $I_{RMS}$ = 8.61 A for SS Sarajevo 1 - Sarajevo 20, overhead lines are used as input parameters for magnetic flux density estimation.

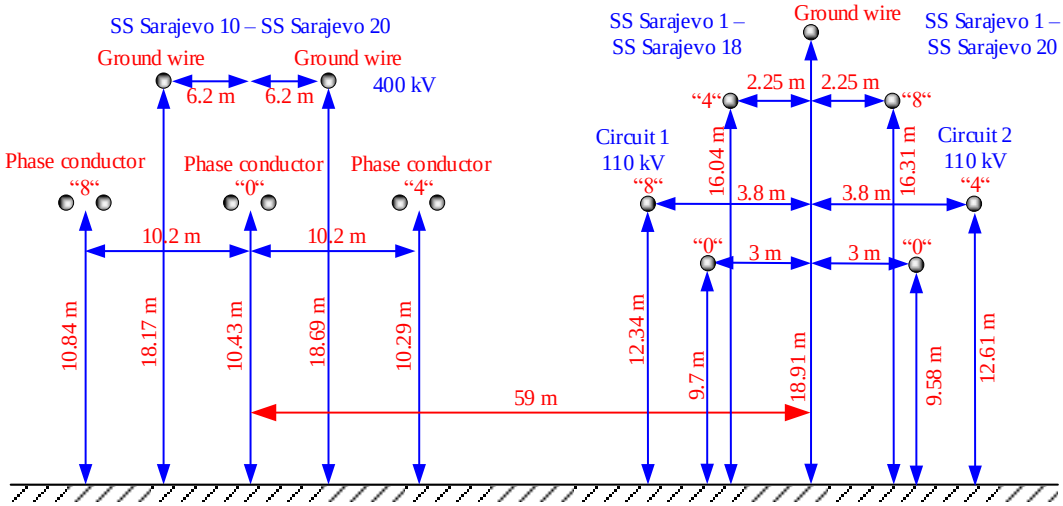


**Fig. 5.** Configuration of 400 kV and 2×110 kV overhead lines sharing common corridor

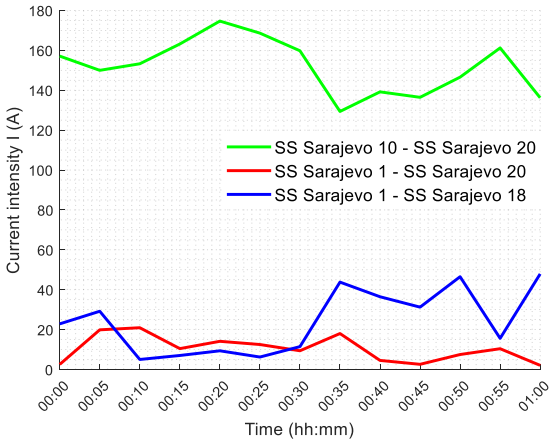


**Fig. 6.** Phase currents during the measurements for the overhead lines that share a common corridor

Magnetic flux density distributions under the overhead lines that share a common corridor are shown in Fig. 7.

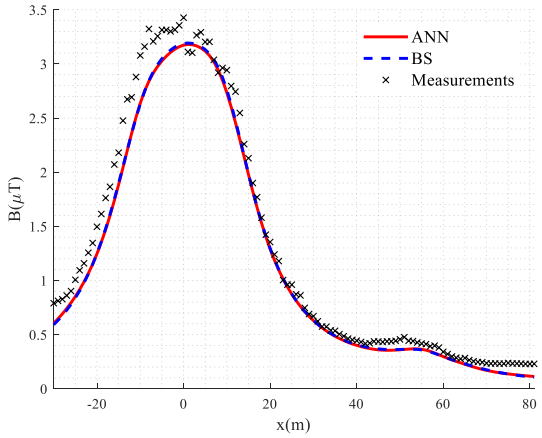


**Fig. 7.** Magnetic flux density distribution under 400 kV and 2×110 kV overhead lines that share a common corridor

Results presented in Fig. 7 show that there is a close match between the results obtained by the ANN based method and BS law-based method over the entire lateral profile. Furthermore, these results are in good agreement with magnetic flux density measurements results.

### 3.3 Validation on a large dataset of field measurements

In addition to the magnetic flux density measurements near overhead lines presented in this paper, measurements were also made near other configurations of single-circuit and multi-circuit overhead lines. In this way, representative datasets were formed, on the basis of which the validation of the ANN-based method for magnetic flux density estimation can be carried out in a credible way. Validation was carried out in an identical way for single-circuit and multi-circuit overhead lines. Regardless, at all points where the measurements were made, for the considered configurations of the overhead lines and their load conditions during the measurement, the magnetic flux density was determined using the considered ANN-based method. In total, 809 measurement points under different configurations of single-circuit overhead lines are considered. The scatter plot in Fig. 8 shows the agreement between measurements and ANN-based estimation results, for single-circuit overhead lines. An ideal case where results are identical is represented with the red line.

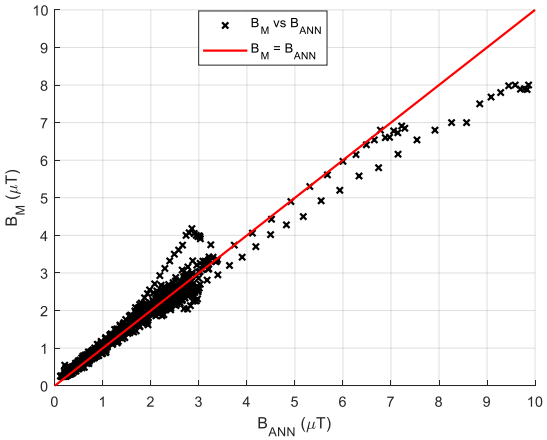


**Fig. 8.** Comparison of ANN-based method and measurements results for single-circuit overhead lines

For multi-circuit overhead lines or overhead lines that share common corridors, 451 measurement points are considered. In Fig. 9, a scatter plot demonstrates the agreement between measurement results and ANN-based method estimates. As in the previous case, the ideal case is represented by the red line.

Despite the different sources of measurements or estimation errors, it can be observed from Figs. 8 and 9 that there are no significant differences between results obtained by different methods. The magnetic flux density values obtained by the ANN-based method and field measurements, in all cases considered in this paper, are below the reference values defined by the literature presented in the introductory section. This statement is valid for both occupational and general public exposure.

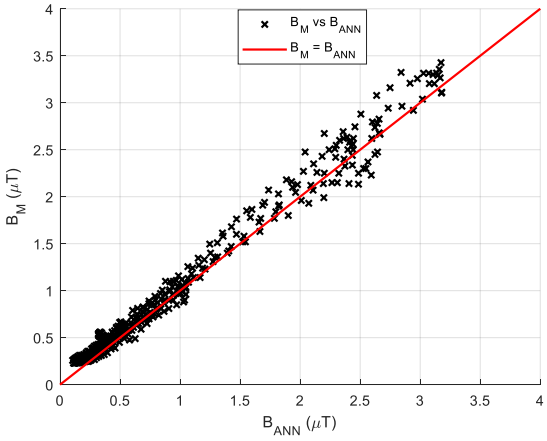


**Fig. 9.** Comparison of ANN-based method and measurements results for multi-circuit overhead lines

In addition to the visual comparison of the magnetic flux density measurements and estimation results, quantitative indicators are used to assess the performance of the ANN-based method for magnetic flux density estimation.

In this paper, the root mean squared error and the coefficient of determination are used to measure how well the observed outcomes are predicted by the ANN-based method. Root mean squared error and coefficient of determination, adjusted to the considered variables, are defined by the following equations [40]:

$$RMSE = \sqrt{\frac{\sum_{m=1}^{M}\left(B_m - \hat{B}_m\right)^2}{M}} \tag{8}$$

$$R^2 = 1 - \frac{\sum_{m=1}^{M}\left(B_m - \hat{B}_m\right)^2}{\sum_{m=1}^{M}(B_m - \bar{B})^2} \tag{9}$$

where RMSE and $R^2$ denote the root mean squared error and the coefficient of determination, respectively, $B_m$ is the $m$-th measured value of magnetic flux density in the dataset, $\hat{B}_m$ is $m$-th estimated value obtained by ANN-based method, $\bar{B}$ is the mean value of measured magnetic flux density values, and $M$ is the total number of the samples in the dataset.

The root mean squared error and coefficient of determination values are calculated according to equations (8) and (9) using the data presented in Figs. 8 and 9. The calculation results are presented in Table 1.

**Table 1.** Quantitative indicators

| Parameters | RMSE | $R^2$ |
|---|---|---|
| Single-circuit overhead lines | 0.3090 | 0.9494 |
| Multi-circuit overhead lines | 0.1288 | 0.9775 |

As it can be noted from results presented in Table 1, in both considered cases values of coefficient of determination are close to the ideal value for this quantitative indicator. Furthermore, low values of root mean squared error are achieved. These results indicate that the considered ANN-based method provides a high degree of agreement with measurement results.

Considering the results presented in Figs. 8 and 9, and also quantitative indicators presented in Table 1 it can be seen that the presented method provides satisfactory magnetic flux density estimation. Also, from the presented results, it can be noted that the ANN-based method shows similar performances for both analyzed cases of single-circuit or multi-circuit overhead lines.

## 4 Discussion

For analyzed scenarios of magnetic flux density distribution over lateral profile under the single-circuit overhead line, and single-circuit and multi-circuit overhead lines that share a common corridor, a good matching between the ANN-based method and BS law based method results are obtained. On the other hand, there are some discrepancies between the magnetic flux density distributions over the lateral profile obtained by these methods and measurement results. The discrepancies can also be noticed if the results of measurements under multiple overhead lines are considered. The main sources of these discrepancies are uneven terrain, errors in phase conductor height measurement, fluctuation of the phase current during magnetic flux density measurement, and asymmetrical current flow through phase conductors. Also, the assumptions under which the method was developed are one of the sources of deviations between calculations and measurement results.

Observing the recorded phase current fluctuations during the measurements, shown in Figs. 3 and 6, it can be noted that they are significant and unpredictable. Although in the case of single-circuit overhead lines, these fluctuations can be compensated, in the case of multi-circuit and/or overhead lines that share common

corridors this is not possible. Phase current fluctuations of each three-phase circuit are independent in relation to the others. Furthermore, the lateral profile length, i.e. the number of measurement points is considerably higher. Thus, the phase current fluctuations during the measurements can be even more significant in this case. In comparison to the case of single-circuit overhead lines, multi-circuit overhead lines are way more challenging. Regardless of that, results obtained by the ANN-based method are in close agreement with measurement results, over the entire considered lateral profile.

The calculations are made for the overhead lines in their normal operating conditions and symmetric phase currents. In such situations there are no current flow trough the ground wires, so their contribution to the overall magnetic flux density distribution is not taken into account. The actual phase currents are obtained from the SCADA system of the transmission system operator of Bosnia and Herzegovina. This SCADA system does not provide phase currents of each phase, so only one phase current for each overhead line is available. Since all phase currents contribute to the magnetic induction distribution in the vicinity of the overhead line, it could be the source of the error associated with the results. Considering the results presented in Figs. 4 and 7 the phase current asymmetry can be the source of discrepancies between measurements and calculation results. However, as it can be noted from the Figs. 4 and 7, the observed discrepancies are not significant and also can be influenced by the other sources of the errors associated with the measurement procedure or calculation method.

In the literature, authors have proposed different methods for the determination of the magnetic flux density in the vicinity of the overhead lines. Regardless of which method is applied, two different approaches to this problem can be observed. The first approach is to apply 2D models that consider the overhead lines' conductors as infinitely long and ideally parallel with the ground surface. On the other hand, the 3D approaches, take into account the catenary of the overhead line conductors. Magnetic flux density spatial component that is parallel to the phase conductors is significantly smaller than two remaining spatial components. Although the 3D models enable calculation of all magnetic flux density spatial components, they are way more computationally and timely demanding compared to the 2D models [22]. In the most literature and practical applications, 2D models are employed for magnetic flux density determination under overhead lines, so in this paper, the same principle is applied. The presented experimental field measurements are performed with the instrument that indicates the magnetic flux density RMS value taking into account all three spatial components. These results have closely matched the results obtained by the ANN-based method, and the 2D algorithm of the BS law based method. This speaks in favor of the error introduced into the results by applying the 2D model is of little significance.

Overall, although different factors associated with the calculation and measurement results can be the source of the discrepancies between them. The magnetic flux density distributions presented in Figs. 4 and 7 show that a good matching between them is obtained. The limited influence of the previously discussed factors is also confirmed by the magnetic flux density measurements in the vicinity of a large number of different single-circuit and multi-circuit overhead lines, shown in Figs. 8 and 9, as well as the quantitative indicators presented in Table 1.

## 5 Conclusion

The results presented in this paper demonstrate that the considered ANN-based method can be effectively applied to the magnetic flux density determination for arbitrary configurations and load conditions of single-circuit, multi-circuit, and overhead lines that share a common corridor. Validation by comparison with a substantial amount of measurement results obtained for different configurations of overhead lines, and also a comparison with BS law-based method calculation is performed. Validation demonstrates that the ANN-based estimation method can be used to accurately estimate magnetic flux density in the vicinity of overhead lines. The principal advantage of the considered method, besides simple application, is its understandability since it uses physical parameters as its inputs, and basic mathematical operations for ANN model outputs postprocessing. This method is designed to be able to consider arbitrary phase conductor configurations. Furthermore, any overhead line load changes can be effectively considered. This method can be effectively used to analyze the realistic and worst-case scenarios of magnetic flux density exposures in the vicinity of, both existing and new designs of the overhead lines.

The future work will be directed in a developing an ANN-based method considering also the third dimensions, so a substations or other complex objects could be considered. Overhead lines are object where approximation of conductors as infinite long straight wires does not significantly influence the obtained results. However, for cases of more complex objects such approximation could be insufficient. In such cases the ANN-based methodology could provide simplification of the application of such model from the end user perspective, and also reduce demands for computation resources comparing to traditional methods.

## Acknowledgement

This research was supported by the Ministry of Education and Science of the Federation of Bosnia and Herzegovina under the grant 05-35-2496-1/23.

## References

[1] T. Guillod, P. Papamanolis, and J. W. Kolar, “Artificial Neural Network (ANN) Based Fast and Accurate Inductor Modeling and Design,” IEEE Open Journal of Power Electronics, vol. 1, pp. 284–299, 2020.

[2] O. I. Abiodun, A. Jantan, A. E. Omolara, K. V. Dada, N. A. Mohamed, and H. Arshad, “State-of-the-art in artificial neural network applications: A survey,” Heliyon, vol. 4, no. 11, p. e00938, 2018.

[3] E. S. N. R. Paidi, H. Marzooghi, J. Yu, and V. Terzija, “Development and validation of artificial neural network-based tools for forecasting of power system inertia with wind farms penetration,” IEEE Systems Journal, vol. 14, no. 4, pp. 4978–4989, 2020.

[4] A. Kumbhar, P. G. Dhawale, S. Kumbhar, U. Patil, and P. Magdum, “A comprehensive review: Machine learning and its application in integrated power system,” Energy Reports, vol. 7, pp. 5467–5474, 2021.

[5] A. Khan, V. Ghorbanian, and D. Lowther, “Deep learning for magnetic field estimation,” IEEE Transactions on Magnetics, vol. 55, no. 6, pp. 1–4, 2019.

[6] E. I. Amoiralis, P. S. Georgilakis, T. D. Kefalas, M. A. Tsili, and A. G. Kladas, “Artificial intelligence combined with hybrid fem-be techniques for global transformer optimization,” IEEE Transactions on Magnetics, vol. 43, no. 4, pp. 1633–1636, 2007.

[7] M. S. I. Sagar, H. Ouassal, A. I. Omi, A. Wisniewska, H. M. Jalajamony, R. E. Fernandez, and P. K. Sekhar, “Application of machine learning in electromagnetics: Mini-review,” Electronics, vol. 10, no. 22, 2021.

[8] V. T. Nguyen, S. Bollmann, M. Bermingham, and M. S. Dargusch, “Efficient modelling of permanent magnet field distribution for deep learning applications,” Journal of Magnetism and Magnetic Materials, vol. 559, p. 169521, 2022.

[9] M. Baldan, G. Baldan, and B. Nacke, “Solving 1d non-linear magneto quasi-static maxwell’s equations using neural networks,” IET Science, Measurement & Technology, vol. 15, no. 2, pp. 204–217, 2021.

[10] S. Pollok and R. Bjørk, “Deep learning for magnetism,” Europhysics News, vol. 53, no. 2, pp. 18–21, 2022.

[11] M. Bonato, E. Chiaramello, M. Parazzini, P. Gajšek, and P. Ravazzani, “Extremely low frequency electric and magnetic fields exposure: Survey of recent findings,” IEEE Journal of Electromagnetics, RF and Microwaves in Medicine and Biology, pp. 1–13, 2023

[12] D. Poljak and M. Cvetkovic, Human Interaction with Electromagnetic Fields: Computational Models in Dosimetry. Academic Press, 2019.

[13] C. Gonzalez, A. Peratta, and D. Poljak, “Pregnant woman exposed to extremely low frequency electromagnetic fields,” in 2008 16th Inter- national Conference on Software, Telecommunications and Computer Networks, 2008, pp. 11–15.

[14] Directive European Council, “Council Recommendation of 12 July 1999 on the limitation of exposure of the general public to electromagnetic fields (0 Hz to 300 GHz) 1999/519.”

[15] J. Lin, R. Saunders, K. Schulmeister, P. Söderberg, B. Stuck, A. Swerdlow, et al., "ICNIRP guidelines for limiting exposure to time-varying electric and magnetic fields (1 Hz to 100 kHz)", 2010, *Health Phys.*, vol. 99, no. 6, pp. 818-836.

[16] G. Mazzanti, “Evaluation of continuous exposure to magnetic field from ac overhead transmission lines via historical load databases: Common procedures and innovative heuristic formulas,” IEEE Transactions on Power Delivery, vol. 25, no. 1, pp. 238–247, 2010.

[17] European Parliament, “Directive 2013/35/EU of the European Parliament and of the council of 26 June 2013 on the minimum health and safety requirements regarding the exposure of workers to the risks arising from physical agents (electromagnetic fields) (20th individual Directive within the meaning of Article 16 (1) of Directive 89/391/EEC) and repealing Directive 2004/40/EC,” Official Journal of the European Union L, vol. 179, 2013.

[18] R. Stam, “Comparison of international policies on electro-magnetic fields:(power frequency and radiofrequency fields),” 2018.

[19] "IEEE Standard for Safety Levels with Respect to Human Exposure to Electric Magnetic and Electromagnetic Fields 0 Hz to 300 GHz", IEEE Std C95.1-2019 (Revision of IEEE Std C95.1-2005/ Incorporates IEEE Std C95.1-2019/Cor 1-2019), 2019, pp. 1-312.

[20] J. Bendik, M. Cenky, Z. Eleschova, A. Belan, and B. Cintula, “Influence of the harmonic content on the root mean square value of the electro- magnetic field produced by overhead power lines,” in 14th International Scientific Conference on Energy Ecology Economy (EEE) Conference Location Slovakia, 2018, pp. 116–119.

[21] J. Salari, A. Mpalantinos, and J. Silva, “Comparative analysis of 2- and 3-d methods for computing electric and magnetic fields generated by overhead transmission lines,” IEEE Transactions on Power Delivery, vol. 24, pp. 338 – 344, 2009.

[22] A. Z. El Dein, “Magnetic-Field Calculation Under EHV Transmission Lines for More Realistic Cases,” IEEE Transactions on Power Delivery, vol. 24, no. 4, pp. 2214–2222, 2009.

[23] J. Bendík, M. Cenký, Ž. Eleschová, et al. Comparison of electromagnetic fields emitted by typical overhead power line towers. Electr Eng 103, 1019–1030 (2021).

[24] S. Vornicu, E. Lunca, B. C. Neagu, and F. C. Baiceanu, “Assessment of extremely low-frequency magnetic field from multiple high-voltage overhead power lines in parallel configuration,” in 2022 International Conference and Exposition on Electrical And Power Engineering (EPE), 2022, pp. 723–726.

[25] I. Pavel, C. Petrescu, V. David, and E. Lunca, “Estimation of the spatial and temporal distribution of magnetic fields around overhead power lines—a case study,” Mathematics, vol. 11, p. 2292, 2023.

[26] C. A. Belhadj and S. El-Ferik, "Electric and Magnetic Fields Estimation for Live Transmission Line Right of Way Workers Using Artificial Neural Network," 2009 15th International Conference on Intelligent System Applications to Power Systems, Curitiba, Brazil, 2009, pp. 1-6,

[27] V. Ranković and J. Radulović, “Prediction of magnetic field near power lines by normalized radial basis function network,” Advances in Engineering Software, vol. 42, no. 11, pp. 934 – 938, 2011.

[28] A. Alihodzic, A. Mujezinovic, and E. Turajlic, “Electric and Magnetic Field Estimation Under Overhead Transmission Lines Using Artificial Neural Networks,” IEEE Access, vol. 9, pp. 105 876–105 891, 2021.

[29] R Gallego-Martínez, F.J. Muñoz-Gutiérrez, A Rodríguez-Gómez, “Trajectory optimization for exposure to minimal electromagnetic pol- lution using genetic algorithms approach: A case study,” Expert Systems with Applications, vol. 207, p. 118088, 2022.

[30] H. Carlak, S. Ozen, and S. Bilgin, “Low-frequency exposure analysis using electric and magnetic field measurements and predictions in the proximity of power transmission lines in urban areas,” Turkish Journal of Electrical Engineering & Computer Sciences, vol. 25, pp. 3994–4005, 2017.

[31] A. Mujezinovic, E. Turajlic, A. Alihodzic, N. Dautbasic, and M. M. Dedovic, “Novel method for magnetic flux density estimation in the vicinity of multi-circuit overhead transmission lines,” IEEE Access, vol. 10, pp. 18 169–18 181, 2022.

[32] E. Turajlic, A. Alihodzic, and A. Mujezinovic, “Artificial neural network models for estimation of electric field intensity and magnetic flux density in the proximity of overhead transmission line,” Radiation Protection Dosimetry, vol. 199, no. 2, pp. 107–115, 11 2023.

[33] “IEC 62110:2009 Electric and magnetic field levels generated by AC power systems - Measurement procedures with regard to public expo- sure,” International Electrotechnical Commission, 2009.

[34] “IEEE Standard Procedures for Measurement of Power Frequency Electric and Magnetic Fields from AC Power Lines,” IEEE Std 644- 2019 (Revision of IEEE Std 644-2008), pp. 1–40, 2020.

M. Møller, “A Scaled Conjugate Gradient Algorithm for Fast Super- vised Learning. Neural Networks,” Neural Networks, vol. 6, pp. 525– 533, 12. 1993.

[36] E. Lunca, S. Ursache, and A. Salceanu, “Computation and analysis of the extremely low frequency electric and magnetic fields generated by two designs of 400 kv overhead transmission lines,” Measurement, vol. 124, pp. 197–204, 2018.

[37] C. Nicolaou, A. Papadakis, P. Razis, G. Kyriacou, and J. Sahalos, “Measurements and predictions of electric and magnetic fields from power lines,” Electric Power Systems Research, vol. 81, pp. 1107–1116, 2011.

[38] “IEC 61786-2:2014 - Measurement of DC magnetic, AC magnetic and AC electric fields from 1 Hz to 100 kHz with regard to exposure of human beings - Part 2: Basic standard for measurements,” International Electrotechnical Commission, 2014.

[39] https://www.narda-sts.com/en/wideband-emf/ elt-400/

[40] M. Peng, A. V. Nguyen, J. Wang, and R. Miller, “A critical review of the model fitting quality and parameter stability of equilibrium adsorption models,” Advances in Colloid and Interface Science, vol. 262, pp. pp. 50–68, 2018.

Received 23 February 2024